



Article

Anti-HER2 Cancer-Specific mAb, H₂Mab-250-hG₁, Possesses Higher Complement-Dependent Cytotoxicity than Trastuzumab

Hiroyuki Suzuki ¹, Tomokazu Ohishi ^{2,3}, Tomohiro Tanaka ¹, Mika K. Kaneko ¹ and Yukinari Kato ^{1,*}

¹ Department of Antibody Drug Development, Tohoku University Graduate School of Medicine, 2-1 Seiryō-machi, Aoba-ku, Sendai 980-8575, Japan; hiroyuki.suzuki.b4@tohoku.ac.jp (H.S.); tomohiro.tanaka.b5@tohoku.ac.jp (T.T.); mika.kaneko.d4@tohoku.ac.jp (M.K.K.)

² Institute of Microbial Chemistry (BIKAKEN), Numazu, Microbial Chemistry Research Foundation, 18-24 Miyamoto, Numazu-shi, Shizuoka 410-0301, Japan; ohishit@bikaken.or.jp

³ Institute of Microbial Chemistry (BIKAKEN), Laboratory of Oncology, Microbial Chemistry Research Foundation, 3-14-23 Kamiosaki, Shinagawa-ku, Tokyo 141-0021, Japan

* Correspondence: yukinari.kato.e6@tohoku.ac.jp; Tel.: +81-22-717-8207

Abstract: Cancer-specific monoclonal antibodies (CasMabs) that recognize cancer-specific antigens with in vivo antitumor efficacy are innovative therapeutic strategies for minimizing adverse effects. We previously established a cancer-specific anti-human epidermal growth factor receptor 2 (HER2) monoclonal antibody (mAb), H₂Mab-250/H₂CasMab-2. In flow cytometry and immunohistochemistry, H₂Mab-250 reacted with HER2-positive breast cancer cells but did not show reactivity to normal epithelial cells. In contrast, a clinically approved anti-HER2 mAb, trastuzumab, strongly recognizes both breast cancer and normal epithelial cells in flow cytometry. The human IgG₁ version of H₂Mab-250 (H₂Mab-250-hG₁) possesses compatible in vivo antitumor effects against breast cancer xenografts to trastuzumab despite the lower affinity and effector activation than trastuzumab in vitro. This study compared the antibody-dependent cellular cytotoxicity (ADCC) and complement-dependent cellular cytotoxicity (CDC) between H₂Mab-250-hG₁ and trastuzumab. Both H₂Mab-250-hG₁ and trastuzumab showed ADCC activity against HER2-overexpressed Chinese hamster ovary -K1 and breast cancer cell lines (BT-474 and SK-BR-3) in the presence of human natural killer cells. Some tendency was observed where trastuzumab showed a more significant ADCC effect compared to H₂Mab-250-hG₁. Importantly, H₂Mab-250-hG₁ exhibited superior CDC activity in these cells compared to trastuzumab. Similar results were obtained in the mouse IgG_{2a} types of both H₂Mab-250 and trastuzumab. These results suggest the different contributions of ADCC and CDC activities to the antitumor effects of H₂Mab-250-hG₁ and trastuzumab, and indicate a future direction for the clinical development of H₂Mab-250-hG₁ against HER2-positive tumors.

Keywords: HER2; cancer-specific monoclonal antibody; antitumor effect; complement-dependent cellular cytotoxicity



Citation: Suzuki, H.; Ohishi, T.; Tanaka, T.; Kaneko, M.K.; Kato, Y. Anti-HER2 Cancer-Specific mAb, H₂Mab-250-hG₁, Possesses Higher Complement-Dependent Cytotoxicity than Trastuzumab. *Int. J. Mol. Sci.* **2024**, *25*, 8386. <https://doi.org/10.3390/ijms25158386>

Academic Editors: Yong-Seok Heo, Hisashi Harada, Stergios Boussios and Matin Sheriff

Received: 22 April 2024

Revised: 27 July 2024

Accepted: 30 July 2024

Published: 1 August 2024



Copyright: © 2024 by the authors. Licensee MDPI, Basel, Switzerland. This article is an open access article distributed under the terms and conditions of the Creative Commons Attribution (CC BY) license (<https://creativecommons.org/licenses/by/4.0/>).

1. Introduction

Human epidermal growth factor receptor 2 (HER2) is a member of the receptor tyrosine kinases. Heterodimerization of HER2 with other HER family members and the ligands or ligand-independent HER2 homodimerization results in the autophosphorylation of the cytoplasmic domain. This event initiates a variety of signaling, such as the RAS and PI3K pathways, leading to cancer cell proliferation, survival, and invasiveness [1]. The overexpression of HER2 is observed in approximately 20% of breast cancers [2] and 20% of gastric cancers [3], which are associated with higher rates of recurrence and shorter overall survival.

Trastuzumab, an anti-HER2 monoclonal antibody (mAb), exhibited in vitro anti-proliferative efficacy and a potent antitumor effect in vivo [4,5]. The combination of

chemotherapy with trastuzumab in HER2-positive breast cancer patients with metastasis improves the progression-free survival and overall survival [6]. Trastuzumab was approved by the U.S. Food and Drug Administration (FDA) for the treatment of HER2-positive breast cancer [6] and has been the most effective therapy for it for more than 20 years [7]. Trastuzumab is administered in patients with HER2-overexpressed tumors, which are defined by solid and complete membranous staining of more than 10% of cells in immunohistochemistry (IHC 3+) and/or in situ hybridization (ISH)-amplified [8]. Furthermore, trastuzumab–deruxtecan (T-DXd), a trastuzumab-based antibody–drug conjugate (ADC), has been developed and approved by the FDA [9]. T-DXd exhibited superior efficacy in not only HER2-positive breast cancers [10,11] but also HER2-low (IHC 1+ or IHC 2+ /ISH-non-amplified) advanced breast cancers [12] and HER2-mutant lung cancers [13]. Because half of all breast cancers are classifiable as HER2-low, a significant number of patients are estimated to receive the benefit from T-DXd therapy [14].

The immunologic engagement of trastuzumab mediates the clinical efficacy [4]. Antibody-dependent cellular cytotoxicity (ADCC) is elicited by natural killer (NK) cells or macrophages upon the binding of Fcγ receptors (FcγRs) to the Fc region of mAbs [4]. Trastuzumab is a humanized IgG₁ mAb that binds to FcγRs [15] and activates macrophages, neutrophils, and dendritic cells, which change the adaptive immunity by cytokine production, chemotaxis, and antigen presentation [4]. Moreover, the FcγR binding results in the activation of NK cells and macrophages, which can result in the target cell killing [4]. However, the ADCC is impaired by the N-linked glycosylation in the Fc region [16]. In particular, a lack of core fucose on the Fc N-glycan enhances the Fc binding to the FcγRs on effector cells [17]. Therefore, a core fucose deficiency on the Fc N-glycan has been shown to enhance the binding to FcγR on effector cells [17] and exert potent antitumor effects [18]. The defucosylated recombinant mAbs can be produced using fucosyltransferase 8-knockout Chinese hamster ovary (CHO) cells [19].

Complement-dependent cellular cytotoxicity (CDC) is also exerted by the Fc domain of mAbs [20,21]. Although complements have been thought of as an adjunctive component of the antibody-mediated cytolytic effects, complement is currently considered an essential effector of the tumor cytotoxic responses of mAb-based immunotherapy [21]. Through the development of a chimeric anti-CD20 mAb, rituximab, for the treatment of B cell lymphomas, the involvement with the cytolytic capacity of the complement was revealed in the antitumor effect [22,23]. In not only anti-CD20 but also anti-CD38 and CD52 immunotherapies, the cytolytic capacity of the tumor by complements has been shown [23–25]. Furthermore, a growing body of evidence suggests that complements play crucial functions in not only tumor cytolysis but also several immunologic roles in antitumor immunity [26,27]. The crosstalk of complement effectors and cellular signaling pathways influence the T and B cell responses, T helper/effector T cell survival, differentiation, and B cell activation.

A common adverse effect of anti-HER2 mAbs and the ADCs is cardiotoxicity [28]. Routine cardiac monitoring is required for patients [29]. Moreover, the lack of cardiac trabeculae is observed in *ErbB2* (ortholog of *HER2*)-knockout mice [30], and the features of dilated cardiomyopathy are observed in ventricular-specific *ErbB2*-knockout mice [31]. These results indicate that HER2 is involved in normal heart development and homeostasis. Therefore, more selective or specific anti-HER2 mAbs against tumors are required to reduce heart failures.

We previously developed cancer-specific anti-HER2 mAbs, H₂Mab-214/H₂CasMab-1 [32] and H₂Mab-250/H₂CasMab-2 [33], from 278 clones of anti-HER2 mAbs using glioblastoma LN229-expressed HER2 as an antigen. Notably, both H₂Mab-214 and H₂Mab-250 did not react with spontaneously immortalized normal epithelial cells (HaCaT and MCF 10A) [32,33]. Moreover, H₂Mab-250 did not react with immortalized normal epithelial cells derived from the mammary gland, lung bronchus, gingiva, kidney proximal tubule, thymus, corneal, and colon [33]. In contrast, most anti-HER2 mAbs, including trastuzumab, reacted with both cancer and normal epithelial cells [34]. The epitope mapping revealed

that the Trp614 in the HER2 extracellular domain (ECD) 4 mainly contributes to the recognition by H₂Mab-250 [33]. H₂Mab-214 also recognized a similar epitope of H₂Mab-250, and the crystal structure suggests that H₂Mab-214 recognizes a structurally misfolded region in the HER2-ECD4, which usually forms a β -sheet [32]. The result indicates that the local misfolding in the Cys-rich-ECD4 governs the cancer-specificity of H₂Mab-214. Furthermore, we produced mouse IgG_{2a}-type and human IgG₁-type mAbs from H₂Mab-214 and H₂Mab-250. We found that both H₂Mab-214 and H₂Mab-250 possess a compatible *in vivo* antitumor effect against breast cancer xenografts with trastuzumab despite the lower affinity and effector activation than trastuzumab *in vitro* [32,34].

This study compared the ADCC and CDC between H₂Mab-250 and trastuzumab against HER2-overexpressed CHO-K1 (CHO/HER2) and breast cancer cell lines.

2. Results

2.1. ADCC and CDC of H₂Mab-250 and Trastuzumab against Breast Cancers

H₂Mab-250 recognized HER2-positive breast cancers (BT-474 and SK-BR-3) but did not recognize HER2 in normal epithelial cells. In contrast, trastuzumab recognized both types of HER2 [34]. Because H₂Mab-250 and trastuzumab are mouse IgG₁ and human IgG₁, respectively, we produced the human IgG₁ type of recombinant H₂Mab-250 (H₂Mab-250-hG₁) and trastuzumab and confirmed the reactivity against breast cancers and normal epithelial cells (Supplementary Figure S1). Although H₂Mab-250 possesses ~10-fold lower affinity than trastuzumab, H₂Mab-250-hG₁ possesses compatible antitumor effects against BT-474 and SK-BR-3 xenografts compared to trastuzumab [34]. To reveal the contribution of the ADCC and CDC activities to the antitumor effects, we performed an *in vitro* ADCC and CDC assay. Both BT-474 and SK-BR-3 cells were labeled with Calcein-AM. Then, the calcein release was measured due to the cytotoxicity of mAbs plus human NK cell (ADCC) or mAbs plus complements (CDC). As shown in Figure 1A, both H₂Mab-250-hG₁ and trastuzumab induced ADCC against BT-474 cells (47% and 64% cytotoxicity, respectively) more effectively than the control human IgG (20% cytotoxicity; $p < 0.01$). Furthermore, trastuzumab showed a superior ADCC compared to H₂Mab-250-hG₁ ($p < 0.01$). In contrast, H₂Mab-250-hG₁ showed a significant CDC (47% cytotoxicity) compared to the control human IgG (20% cytotoxicity; $p < 0.05$). However, trastuzumab did not show a significant CDC (Figure 1B). In SK-BR-3, both H₂Mab-250-hG₁ and trastuzumab induced ADCC (12% and 17% cytotoxicity, respectively) more effectively than the control human IgG (4% cytotoxicity; $p < 0.05$ and $p < 0.01$, respectively, Figure 1C). Moreover, both H₂Mab-250-hG₁ and trastuzumab exhibited CDC (42% and 26% cytotoxicity, respectively) more effectively than the control human IgG (6% cytotoxicity; $p < 0.01$, Figure 1D). Importantly, H₂Mab-250-hG₁ showed a superior CDC compared to trastuzumab ($p < 0.01$, Figure 1D). These results suggest the different contributions of ADCC and CDC to the antitumor effects of H₂Mab-250-hG₁ and trastuzumab.

2.2. ADCC and CDC by H₂Mab-250 and Trastuzumab against CHO/HER2

To confirm the requirement of HER2 in the ADCC and CDC of H₂Mab-250 and trastuzumab, we used CHO-K1 and CHO/HER2 and performed the ADCC and CDC assays. CHO/HER2 was also recognized by H₂Mab-250 and trastuzumab with low and high reactivity, respectively [34]. As shown in Figure 2A, both H₂Mab-250-hG₁ and trastuzumab induced ADCC against CHO/HER2 cells (70% and 77% cytotoxicity, respectively) more effectively than the control human IgG (13% cytotoxicity; $p < 0.01$). In contrast, H₂Mab-250-hG₁ showed a significant CDC (63% cytotoxicity) compared to the control human IgG (10% cytotoxicity; $p < 0.01$, Figure 2B). However, trastuzumab did not show a significant CDC (Figure 2B). In CHO-K1, we did not observe ADCC and CDC in the presence of H₂Mab-250 and trastuzumab (Figure 2C,D). These results indicate that the recognition of HER2 is essential to the exertion of ADCC and CDC by H₂Mab-250-hG₁ and trastuzumab. Furthermore, dose-dependent activation of CDC activity by H₂Mab-250 and trastuzumab was observed against CHO/HER2, but not CHO-K1 (Figure 2E). H₂Mab-250-hG₁ exhibited

a significant CDC compared to the control human IgG from 25 $\mu\text{g}/\text{mL}$ and showed it compared to trastuzumab at 100 $\mu\text{g}/\text{mL}$ (Figure 2E).

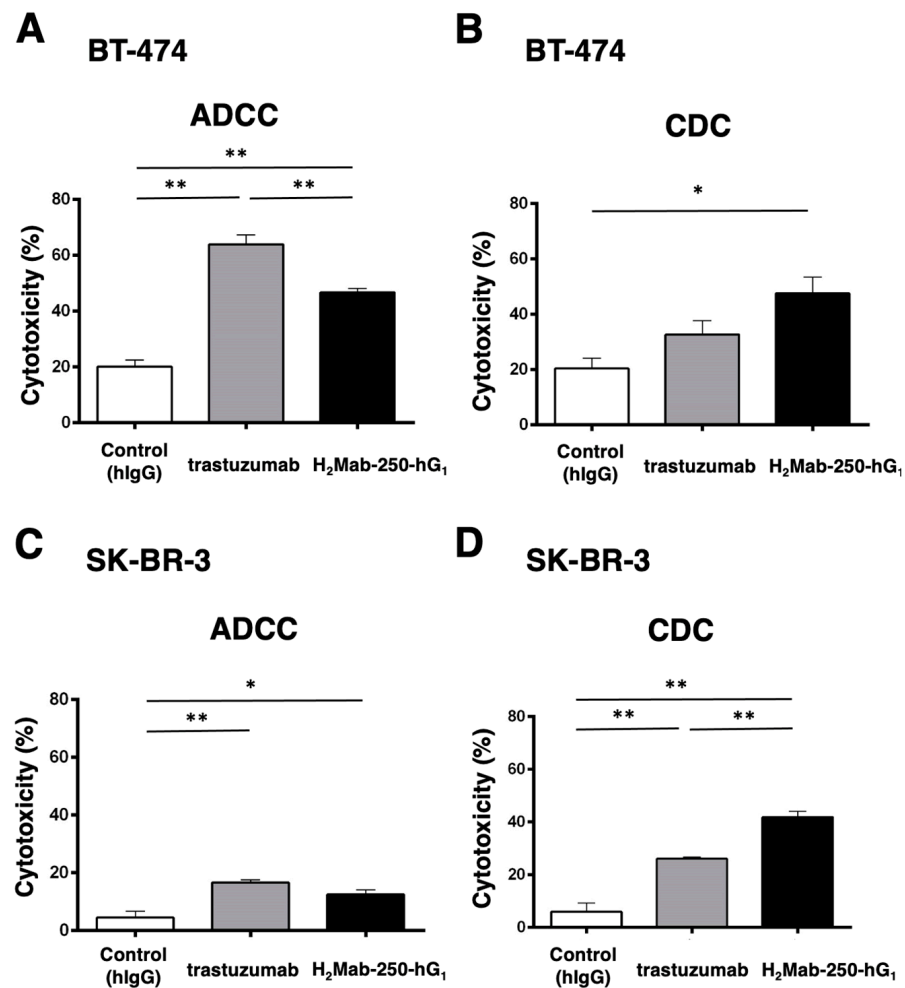


Figure 1. The ADCC and CDC activities were mediated by H₂Mab-250-hG₁ and trastuzumab in BT-474 and SK-BR-3 cells. (A,C) The ADCC induced by human NK cells in the presence of H₂Mab-250-hG₁, trastuzumab, or control human IgG (hIgG) against BT-474 (A) and SK-BR-3 (C) cells. (B,D) The CDC induced by complements in the presence of 100 $\mu\text{g}/\text{mL}$ of H₂Mab-250-hG₁, trastuzumab, or control human IgG against BT-474 (B) and SK-BR-3 (D) cells. Values are shown as the mean \pm SEM. Asterisks indicate statistical significance (** $p < 0.01$ and * $p < 0.05$; one-way ANOVA and Tukey's multiple comparisons test).

2.3. Antitumor Activities by H₂Mab-250-hG₁ and Trastuzumab

Next, we examined the in vivo antitumor efficacy of H₂Mab-250-hG₁ and trastuzumab in the CHO/HER2 xenograft model. We injected H₂Mab-250-hG₁, trastuzumab, and control human IgG intraperitoneally on days 7, 14, and 21 after inoculating CHO/HER2. Furthermore, human NK cells were injected around the tumors on the same days of the Abs injection. Following the inoculation, we measured the tumor volume on days 7, 14, 21, and 28. The H₂Mab-250-hG₁ and trastuzumab administration led to a significant and similar reduction in the CHO/HER2 xenograft on day 28 ($p < 0.01$) compared with that of the control (Figure 3A). Both H₂Mab-250-hG₁ and trastuzumab administration resulted in an 81% reduction in the CHO/HER2 xenograft volume compared with the control human IgG on day 28.

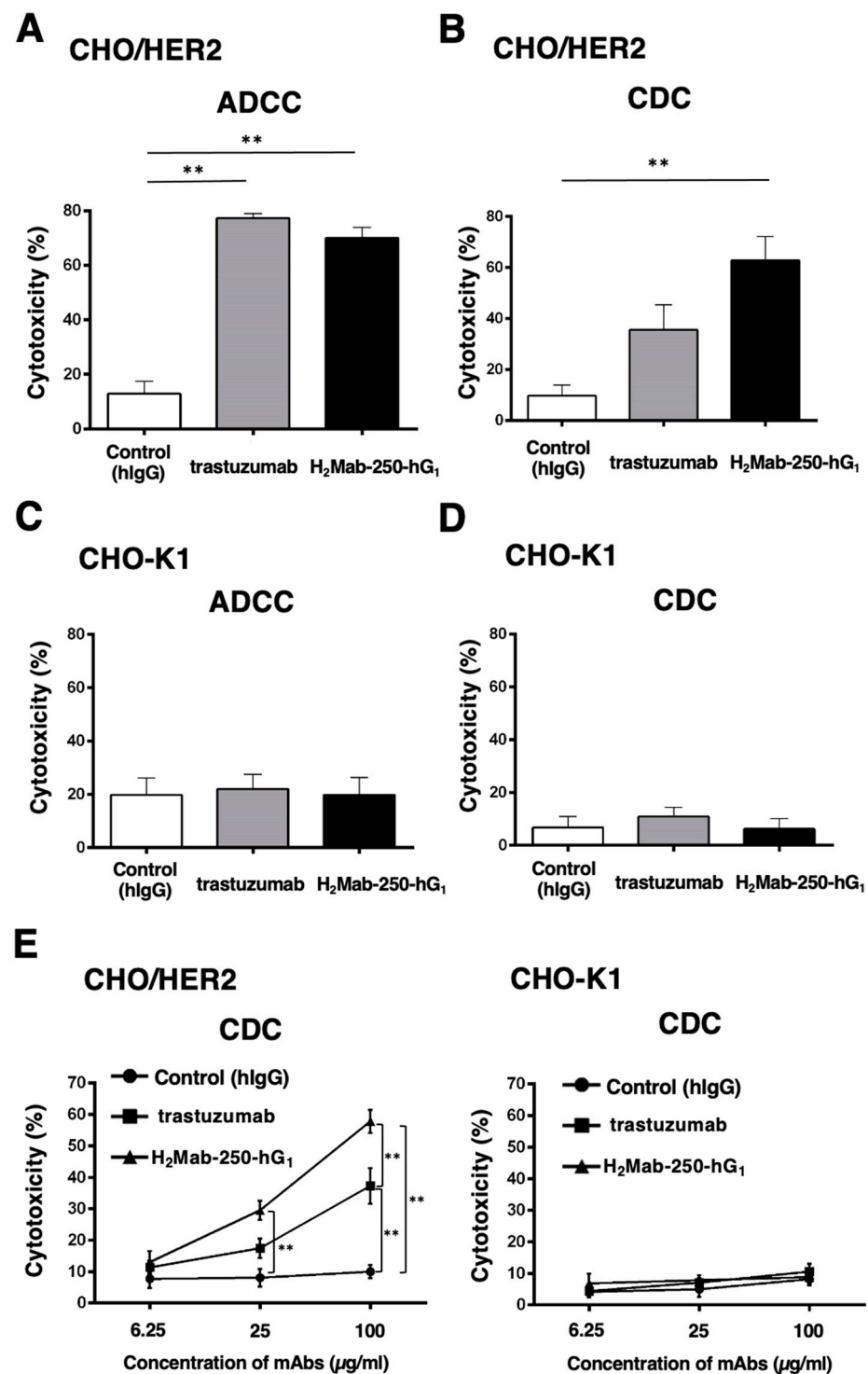


Figure 2. The ADCC and CDC activities are mediated by H₂Mab-250-hG₁ and trastuzumab in CHO/HER2 and CHO-K1 cells. (A,C) The ADCC induced by human NK cells in the presence of H₂Mab-250-hG₁, trastuzumab, or control human IgG (hIgG) against CHO/HER2 (A) and CHO-K1 (C) cells. (B,D) The CDC induced by complements in the presence of 100 μg/mL of H₂Mab-250-hG₁, trastuzumab, or control hIgG against CHO/HER2 (B) and CHO-K1 (D) cells. Values are shown as the mean ± SEM. Asterisks indicate statistical significance (** *p* < 0.01; one-way ANOVA and Tukey's multiple comparisons test). (E) The CDC induced by complements in the presence of 6.25, 25, and 100 μg/mL of H₂Mab-250-hG₁, trastuzumab, or hIgG. Values are shown as the mean ± SEM. Asterisks indicate statistical significance (** *p* < 0.01; two-way ANOVA and Tukey's multiple comparisons test).

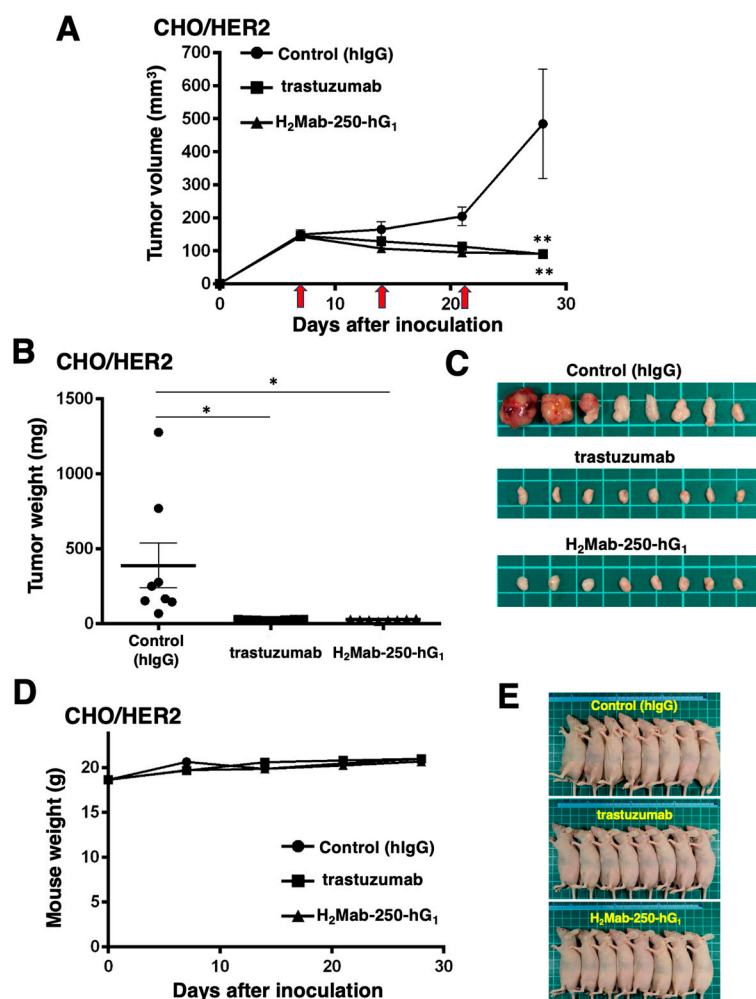


Figure 3. Antitumor activity of H₂Mab-250-hG₁ and trastuzumab against CHO/HER2 xenografts. (A) CHO/HER2 cells (5×10^6 cells) were injected subcutaneously into the left flank of BALB/c nude mice (day 0). On day 7, 100 μ g of H₂Mab-250-hG₁ (n = 8), trastuzumab (n = 8), or control human IgG (hIgG) (n = 8) was injected into the mice. On days 14 and 21, additional antibodies were injected. Human NK cells were injected around the tumors on the same days as the Ab administration (arrows). The tumor volume was measured on days 7, 14, 21, and 28. Values are presented as the mean \pm SEM. ** $p < 0.01$ (two-way ANOVA and Tukey's multiple comparisons test). The tumor weight (B) and appearance (C) of excised CHO/HER2 xenografts on day 28. Values are presented as the mean \pm SEM. * $p < 0.05$ (two-way ANOVA and Tukey's multiple comparisons test). The body weight (D) and appearance (E) of the xenograft-bearing mice treated with trastuzumab, H₂Mab-250-hG₁, or a control hIgG.

The CHO/HER2 xenografts from the H₂Mab-250-hG₁- and trastuzumab-treated mice weighed significantly less than those from the control human IgG-treated mice (93% and 94% reduction, respectively; $p < 0.05$, Figure 3B,C). There was no significant difference between the H₂Mab-250-hG₁- and trastuzumab-treated xenografts.

A body weight loss was not observed in the H₂Mab-250-hG₁- and trastuzumab-treated CHO/HER2 xenograft-bearing mice (Figure 3D), and there was no difference in the body appearance in those mice (Figure 3E).

We also investigated the pharmacokinetics of H₂Mab-250-hG₁ and trastuzumab after administration in nude mice. As shown in Supplementary Figure S2, the half-lives of H₂Mab-250-hG₁ and trastuzumab were determined as 128 and 133 h, respectively. These results indicate that H₂Mab-250-hG₁ possesses a similar half-life compared to trastuzumab.

2.4. ADCC and CDC by Mouse IgG_{2a}-Type H₂Mab-250 and Trastuzumab against CHO/HER2

We next investigated the ADCC and CDC against CHO-K1 and CHO/HER2 using mouse IgG_{2a}-type H₂Mab-250 (H₂Mab-250-mG_{2a}) and trastuzumab (tras-mG_{2a}) to assess the influence of the antibody format. As shown in Figure 4A, tras-mG_{2a} induced ADCC against CHO/HER2 cells (43% cytotoxicity) more effectively than the control mouse IgG_{2a} (10% cytotoxicity; $p < 0.05$). In contrast, H₂Mab-250-mG_{2a} did not significantly induce ADCC against CHO/HER2 cells (Figure 4A). Furthermore, both H₂Mab-250-mG_{2a} and tras-mG_{2a} induced CDC against CHO/HER2 cells (51% and 45% cytotoxicity, respectively) more effectively than the control mouse IgG_{2a} (Figure 4B, 27% cytotoxicity; $p < 0.01$ and $p < 0.05$ respectively). In CHO-K1, we did not observe ADCC and CDC in the presence of H₂Mab-250-mG_{2a} and tras-mG_{2a} (Figure 4C,D).

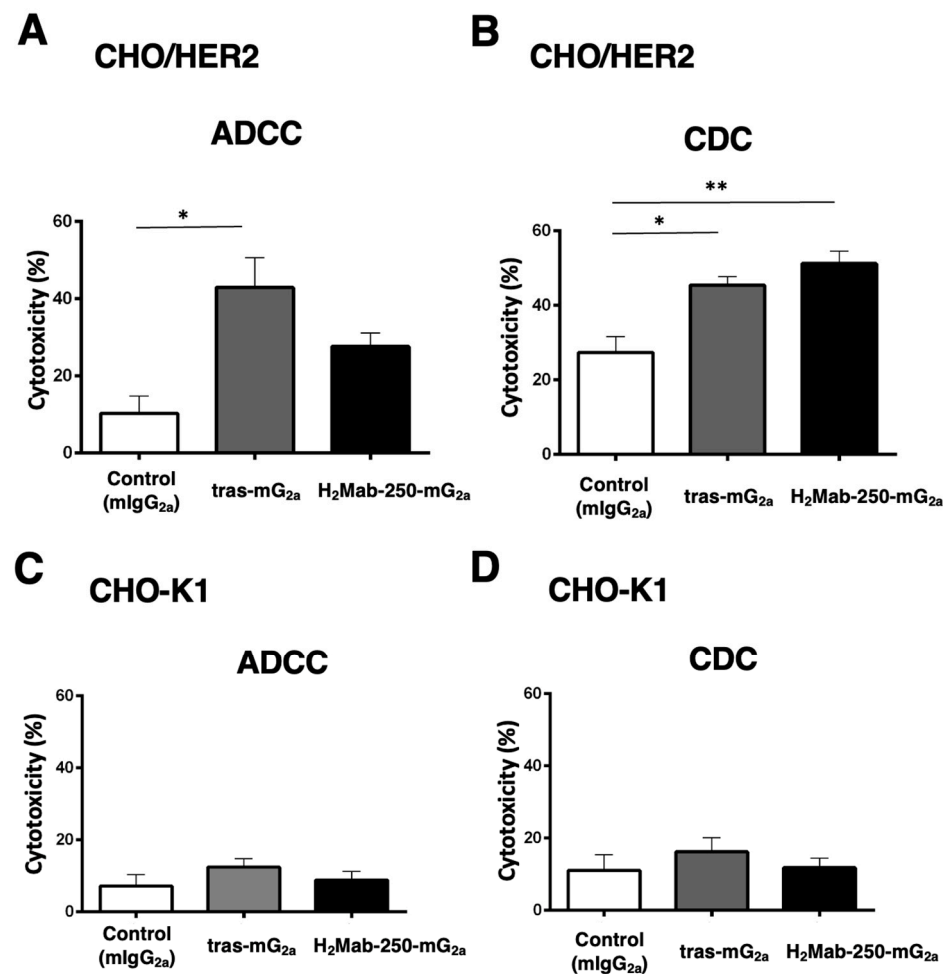


Figure 4. The ADCC and CDC activities are mediated by H₂Mab-250-mG_{2a} and tras-mG_{2a} in CHO/HER2 and CHO-K1 cells. (A,C) The ADCC induced by human NK cells in the presence of 100 µg/mL of H₂Mab-250-mG_{2a}, tras-mG_{2a}, or control mouse IgG_{2a} (mIgG_{2a}) against CHO/HER2 (A) and CHO-K1 (C) cells. (B,D) The CDC induced by complements in the presence of H₂Mab-250-mG_{2a}, tras-mG_{2a}, or control mIgG_{2a} against CHO/HER2 (B) and CHO-K1 (D) cells. Values are shown as the mean ± SEM. Asterisks indicate statistical significance (** $p < 0.01$ and * $p < 0.05$; one-way ANOVA and Tukey's multiple comparisons test).

These results indicate that tras-mG_{2a} showed a superior ADCC compared to H₂Mab-250-mG_{2a}. In contrast, H₂Mab-250-mG_{2a} exhibited a superior CDC to CHO/HER2 compared to tras-mG_{2a}.

2.5. Antitumor Activities by Mouse IgG_{2a}-Type H₂Mab-250 and Trastuzumab

Next, we examined the *in vivo* antitumor efficacy of H₂Mab-250-mG_{2a} and tras-mG_{2a} in the CHO/HER2 xenograft model. We injected H₂Mab-250-mG_{2a}, tras-mG_{2a}, and a control mouse IgG_{2a} intraperitoneally on days 9 and 16 after inoculating CHO/HER2. Following the inoculation, we measured the tumor volume on days 9, 16, and 21. The H₂Mab-250-mG_{2a} and tras-mG_{2a} administration led to a potent and similar reduction in the CHO/HER2 xenograft on days 16 and 21 ($p < 0.01$) compared with that of the control mouse IgG_{2a} (Figure 5A). The H₂Mab-250-mG_{2a} and tras-mG_{2a} administration resulted in a 77% and 74% reduction in the CHO/HER2 xenograft volume compared with the control mouse IgG_{2a} on day 21.

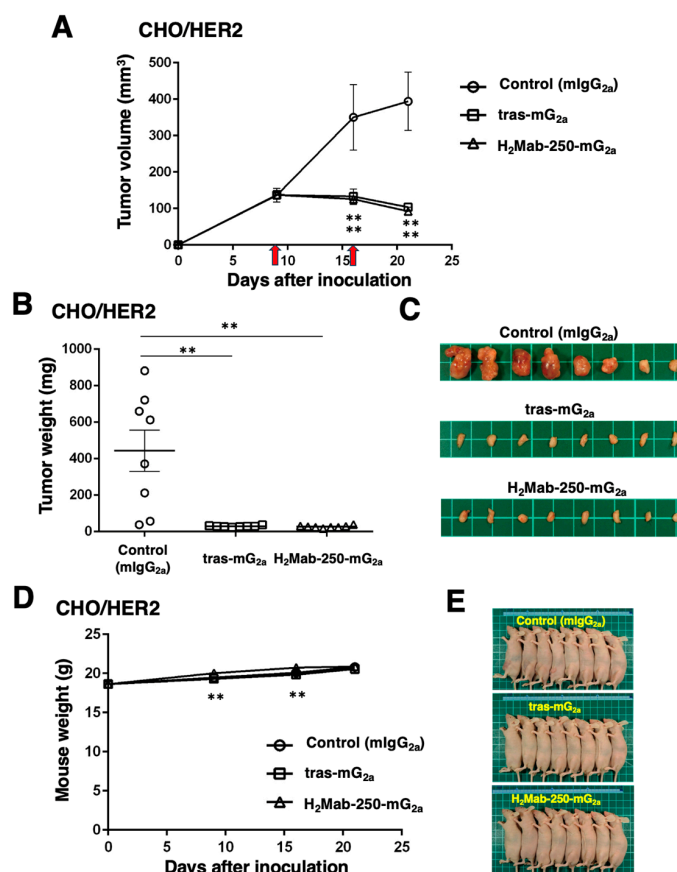


Figure 5. Antitumor activity of H₂Mab-250-mG_{2a} and tras-mG_{2a} against CHO/HER2 xenografts. (A) CHO/HER2 cells (5×10^6 cells) were injected subcutaneously into the left flank of BALB/c nude mice (day 0). On day 9, 100 μ g of H₂Mab-250-mG_{2a} ($n = 8$), tras-mG_{2a} ($n = 8$), or a control mouse IgG_{2a} (mIgG_{2a}) ($n = 8$) was injected into mice. On day 16, additional antibodies were injected (arrows). The tumor volume was measured on days 9, 16, and 21. Values are presented as the mean \pm SEM. ** $p < 0.01$ (two-way ANOVA and Tukey's multiple comparisons test). The tumor weight (B) and appearance (C) of excised CHO/HER2 xenografts on day 21. Values are presented as the mean \pm SEM. ** $p < 0.01$ (two-way ANOVA and Tukey's multiple comparisons test). The body weight (D) and appearance (E) of xenograft-bearing mice treated with H₂Mab-250-mG_{2a} and tras-mG_{2a}, or a control mIgG_{2a}.

The CHO/HER2 xenografts from the H₂Mab-250-mG_{2a}- and tras-mG_{2a}-treated mice weighed significantly less than those from the control mouse IgG_{2a}-treated mice (94% and 94% reduction, respectively; $p < 0.01$, Figure 5B,C). There was no significant difference between the H₂Mab-250-mG_{2a}- and tras-mG_{2a}-treated xenografts.

Figure 5D shows that body weight loss was not observed in the H₂Mab-250-mG_{2a}- and tras-mG_{2a}-treated CHO/HER2 xenograft-bearing mice. However, a slight difference

was observed between the control and H₂Mab-250-mG_{2a}-treated mice. Those mice had no difference in body appearance (Figure 5E).

2.6. Comparison of Antitumor Activities by H₂Mab-250-hG₁ and Trastuzumab in the Absence of Human NK Cells

As shown in Figure 3, we injected human NK cells with H₂Mab-250-hG₁ and trastuzumab because high ADCC activity was expected. Since H₂Mab-250-hG₁ possesses a higher CDC activity, we next compared the antitumor effects of H₂Mab-250-hG₁ and trastuzumab without the human NK cells. We injected H₂Mab-250-hG₁ and trastuzumab intraperitoneally on days 7, 14, and 21 after inoculating CHO/HER2. Following the inoculation, we measured the tumor volume on days 7, 10, 14, 16, 21, 24, and 29. We observed the more potent antitumor efficacy of H₂Mab-250-hG₁ in relation to both the tumor volume ($p < 0.01$, Figure 6A) and weight ($p < 0.01$, Figure 6B) compared with that of trastuzumab at day 29 (Figure 6C).

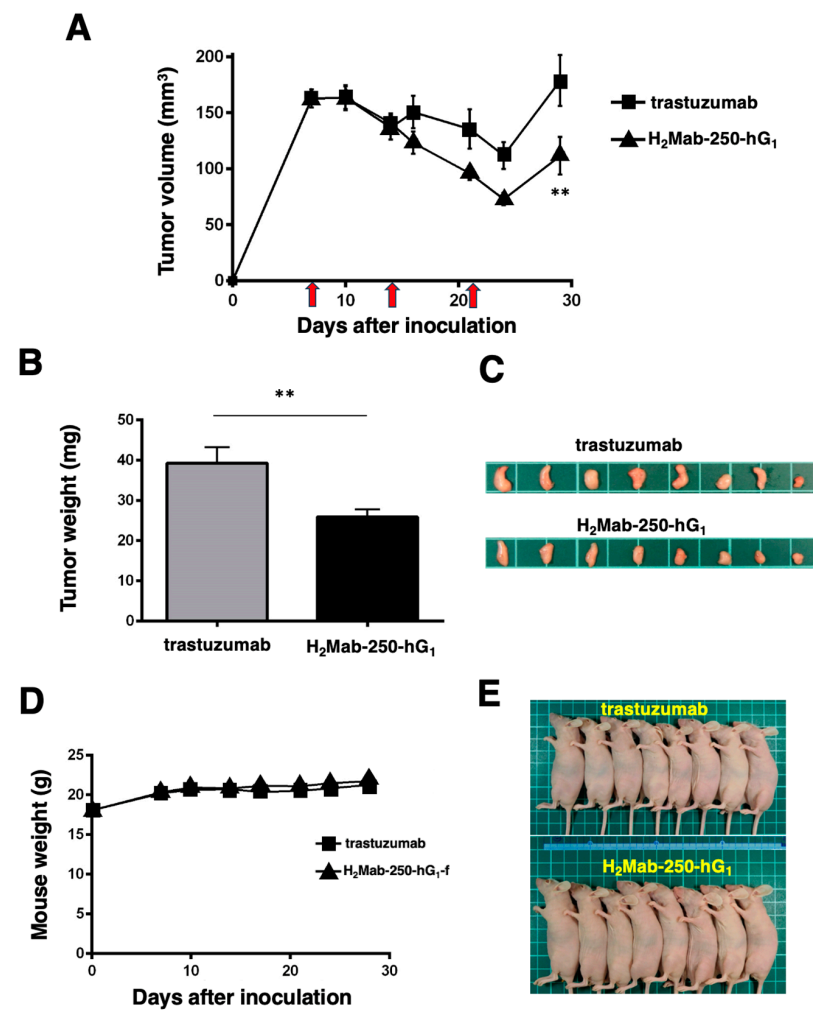


Figure 6. Antitumor activity of H₂Mab-250-hG₁ and trastuzumab against CHO/HER2 xenografts without human NK cell injection. (A) CHO/HER2 cells (5×10^6 cells) were injected subcutaneously into the left flank of BALB/c nude mice (day 0). On day 7, 100 μ g of H₂Mab-250-hG₁ ($n = 8$) or trastuzumab ($n = 8$) was injected into the mice. On days 14 and 21, additional antibodies were injected (arrows). The tumor volume was measured on days 7, 10, 14, 16, 21, 24, and 29. Values are presented as the mean \pm SEM. ** $p < 0.01$ (two-way ANOVA and Tukey's multiple comparisons test). The tumor weight (B) and appearance (C) of the excised CHO/HER2 xenografts on day 29. Values are presented as the mean \pm SEM. ** $p < 0.01$ (two-way ANOVA and Tukey's multiple comparisons test). The body weight (D) and appearance (E) of the xenograft-bearing mice treated with trastuzumab or H₂Mab-250-hG₁.

Body weight loss was not observed in the H₂Mab-250-hG₁- and trastuzumab-treated CHO/HER2 xenograft-bearing mice (Figure 6D), and there was no difference in body appearance in those mice (Figure 6E).

3. Discussion

We have developed CasMabs against HER2 (H₂Mab-250 [33,34]), podocalyxin (PcMab-6 [35]), and podoplanin (LpMab-2 [36] and LpMab-23 [37]) by evaluating the reactivity against cancer and normal cells in flow cytometry and immunohistochemistry. We also showed the *in vivo* antitumor effect of the recombinant mAbs (mouse IgG_{2a} or human IgG₁ types) derived from the abovementioned mAbs [32–34]. Especially, H₂Mab-250 showed a potent antitumor effect *in vivo* [34] despite the lower reactivity and affinity than trastuzumab *in vitro* [33]. However, the reason for this has not been clarified. In this study, we compared the ADCC and CDC activity of H₂Mab-250 and trastuzumab and found that H₂Mab-250 exhibited a superior CDC activity against breast cancer and HER2-overexpressed cells compared to trastuzumab (Figures 1, 2 and 4). Furthermore, both H₂Mab-250-hG₁ and H₂Mab-250-mG_{2a} showed compatible antitumor effects compared to the corresponding isotype of trastuzumab (Figures 3 and 5). These results suggest that the CDC activity of H₂Mab-250 would compensate for the lower ADCC activity in the antitumor efficacy.

Complement is an essential effector of tumor cytotoxic responses in mAb-based immunotherapy [21]. The engagement of the Fc domain of mAbs with complement C1q triggers the assembly of the active C1 complex (C1q, C1r, and C1s), which initiates the cascade. The downstream activation of terminal complement components results in the assembly of the pore-forming membrane attack complex (MAC or C5b–C9) on the tumor cell membrane, which promotes the terminal lytic pathway [21]. Complement activation also leads to tumor cell opsonization by C3-derived opsonins (C3b, iC3b, and C3dg), which bind to the CR3/CR4 complement receptors on phagocytes (neutrophils and macrophages) and augment the FcγR-dependent phagocytic uptake of opsonized tumor cells. Furthermore, complement activation generates pro-inflammatory mediators (C3a and C5a). The anaphylatoxin C5a upregulates the FcγRs on phagocytes and primes them for enhanced phagocytosis and increasing the magnitude of the tumor cytolytic response [21].

Because H₂Mab-250 showed increased CDC activity only in the presence of complement (Figures 1, 2 and 4), the assembly of MAC is thought to be efficiently formed on the cells. Furthermore, the predisposition to CDC of H₂Mab-250 is independent of the isotype or species of mAbs (Figures 2 and 4). Therefore, the complementarity-determining region and epitope of H₂Mab-250 are thought to be necessary. In Figure 6, the antitumor effects of H₂Mab-250-hG₁ were higher than those of trastuzumab without human NK cells, indicating that H₂Mab-250-hG₁ exerts antitumor activities with much higher CDC than trastuzumab *in vivo*. Several factors, including the antigen size and density, determine the engagement of the classical complement pathway. In addition, a geometry of the antigen–mAb complex allows efficient C1q binding [38]. Furthermore, IgG antibodies can form ordered hexamers upon binding to their antigen on cell surfaces. These hexamers efficiently bind the hexavalent complement component C1q, the first step in the classical pathway of complement activation [39,40]. The structure of the H₂Mab-250-HER2 complex may provide adequate access for complements to exert CDC. Further investigation and confirmation are required to clarify the mechanisms of CDC in H₂Mab-250.

Trastuzumab exerts antitumor activity through multiple mechanisms of action but is incapable of eliciting CDC in HER2-positive cancers in the presence of human serum [41,42]. As shown in Figure 1B, trastuzumab did not elicit CDC against BT-474 cells. An anti-HER2 bispecific and biparatopic antibody, zanidatamab, elicited potent CDC against HER2-high tumor cells, including BT-474 cells. Zanidatamab possesses an anti-HER2-ECD4 single-chain variable fragment (scFv) linked to heavy chain 1 and an anti-HER2-ECD2 fragment antigen-binding (Fab) domain on heavy chain 2. Zanidatamab binds adjacent HER2 molecules *in trans* and initiates distinct HER2 reorganization and large HER2 clusters,

which are not observed with trastuzumab [43]. Optimal CDC activity requires hexameric clustering of mAb Fc domains in the mAb–antigen clusters [44]. We identified the epitope of H₂Mab-250 as ₆₁₃-IWKFP-₆₁₇ in the HER2-ECD4. The epitope of trastuzumab is a broader sequence (residues 579–625), which includes the H₂Mab-250 epitope [33]. It is worthwhile to investigate the ability of H₂Mab-250 to form a cluster with HER2.

Chimeric antigen receptor (CAR)-T cell therapy is rapidly advancing as a cancer treatment; however, designing an optimal CAR remains challenging. Due to the specific reactivity against cancer cells, H₂Mab-250 is clinically developed as CAR-T cell therapy, which is evaluated in a phase I study for HER2-positive advanced solid tumors in the US (NCT06241456). We discussed the benefit of reducing CAR affinity to limit trogocytosis, which is observed in the high affinity of CAR-T cells [34]. In the monotherapy of H₂Mab-250, we have reported compatible antitumor effects against breast cancer xenograft compared to trastuzumab [32,34] and showed the importance of CDC in this study. Extensive research indicates that resistance to CDC is induced by the expression of complement regulators in tumor cells during the escape from host immune responses. Notably, an upregulation of the regulators, including CD46, CD55, and CD59, has been shown to prevent CDC through suppression of terminal complement activation and MAC assembly [45–47]. In this regard, several strategies have been developed to overcome the resistance to CDC in mAb-based immunotherapy [48–51]. Therefore, dual targeting of HER2 by H₂Mab-250 and complement regulators should be investigated in future studies in *in vitro* models.

4. Materials and Methods

4.1. Cell Culture

Chinese hamster ovary (CHO)-K1 cells were obtained from the American Type Culture Collection (ATCC, Manassas, VA, USA). CHO-K1 and HER2-overexpressed CHO-K1 (CHO/HER2) [33] were cultured in the Roswell Park Memorial Institute (RPMI)-1640 medium (Nacalai Tesque, Inc., Kyoto, Japan). BT-474 and SK-BR-3 were also obtained from the ATCC, and they were cultured in Dulbecco's Modified Eagle Medium (DMEM) (Nacalai Tesque, Inc.). These media were supplemented with 10% fetal bovine serum (FBS; Thermo Fisher Scientific Inc., Waltham, MA, USA), antibiotic–antimycotic mixed solution (Nacalai Tesque, Inc.). All the cell lines were cultured at 37 °C in a humidified atmosphere with 5% CO₂ and 95% air.

4.2. Production of Recombinant mAbs

To generate H₂Mab-250-hG₁, V_H of H₂Mab-250 and C_H of human IgG₁ were cloned into the pCAG-Ble vector. The V_L of the H₂Mab-250 and C_L of the human kappa light chain were cloned into the pCAG-Neo vector.

To generate H₂Mab-250-mG_{2a}, we cloned the V_H cDNA of H₂Mab-250 and C_H of mouse IgG_{2a} into the pCAG-Ble vector. To generate a mouse IgG_{2a} type of trastuzumab (tras-mG_{2a}), the V_H cDNA of trastuzumab and the C_H cDNA of mouse IgG_{2a} were cloned into the pCAG-Neo vector, and the V_L cDNA of trastuzumab and the C_L cDNA of mouse kappa light chain were cloned into the pCAG-Ble vector.

To generate the control mouse IgG_{2a} (PMab-231), we cloned the heavy and light chains of PMab-231 [52] into the pCAG-Neo and pCAG-Ble vectors, respectively.

The vectors were transfected into BINDS-09 (fucosyltransferase 8-knockout ExpiCHO-S; http://www.med-tohoku-antibody.com/topics/001_paper_cell.htm, accessed on 20 April 2024) cells using the ExpiCHO Expression System (Thermo Fisher Scientific, Inc.) to produce the defucosylated mAbs. The H₂Mab-250-mG_{2a}, tras-mG_{2a}, H₂Mab-250-hG₁, trastuzumab, and PMab-231 were purified using Ab-Capcher (Kagawa, Japan). After washing with PBS, the bound antibodies were eluted with an IgG elution buffer (Thermo Fisher Scientific Inc.) and immediately neutralized using 1 M Tris-HCl (pH 8.0). Finally, the eluates were concentrated using Amicon Ultra (Merck KGaA) and replaced with PBS. The purified mAbs were confirmed by SDS-PAGE in reduced and non-reduced conditions (Supplementary Figure S3).

Normal human IgG was purchased from Sigma-Aldrich Corp. (St. Louis, MO, USA).

4.3. ADCC

The ADCC of H₂Mab-250-hG₁ and trastuzumab was measured as follows. Human NK cells were purchased from Takara Bio, Inc. (Shiga, Japan) and were used as effector cells. The NK cells were used in the following experiment immediately after thawing. We labeled the target cells (BT-474, SK-BR-3, CHO-K1, and CHO/HER2) using 10 µg/mL Calcein AM (Thermo Fisher Scientific, Inc.). The target cells were plated in 96-well plates (1 × 10⁴ cells/well) and mixed with the human NK cells (effector to target ratio, 50:1) and 100 µg/mL of H₂Mab-250-hG₁, trastuzumab or control human IgG. The calcein release was measured after a 4.5 h incubation, and the cytotoxicity (% lysis) was calculated as described previously [34].

The ADCC of H₂Mab-250-mG_{2a} and tras-mG_{2a} was measured as follows. Effector cells were obtained from the spleen of female BALB/c nude mice (Jackson Laboratory Japan, Inc., Kanagawa, Japan). The Calcein AM-labeled target cells (CHO-K1 and CHO/HER2) using 10 µg/mL Calcein AM were plated in 96-well plates (1 × 10⁴ cells/well) and mixed with the effector cells (effector to target ratio, 50:1) with 100 µg/mL of H₂Mab-250-mG_{2a} and tras-mG_{2a} or control mouse IgG_{2a}. After a 4 h incubation at 37 °C, the calcein release into the medium was measured, and the cytotoxicity (% lysis) was calculated.

4.4. CDC

The calcein-labeled target cells (BT-474, SK-BR-3, CHO-K1, and CHO/HER2) were plated and mixed with rabbit complement (final dilution 1:10, or 1:15 [Figure 2E], Low-Tox-M Rabbit Complement; Cedarlane Laboratories, Hornby, ON, Canada) and the indicated concentration of H₂Mab-250-hG₁, trastuzumab or control human IgG. Following incubation for 4.5 h at 37 °C, the calcein released into the medium was measured, as described above. In the case of H₂Mab-250-mG_{2a} and tras-mG_{2a} or control mouse IgG_{2a}, we performed a 4 h incubation at 37 °C and the cytotoxicity (% lysis) was calculated.

4.5. Antitumor Activities of H₂Mab-250-hG₁, Trastuzumab, H₂Mab-250-mG_{2a}, and Tras-mG_{2a}, in Tumor Xenograft Models

To examine the antitumor effect of H₂Mab-250-hG₁, trastuzumab, H₂Mab-250-mG_{2a}, and tras-mG_{2a}, animal experiments were approved by the Institutional Committee for Experiments of the Institute of Microbial Chemistry (approval no. 2023-066 and 2023-074). We determined the body weight loss exceeding 25% and maximum tumor size exceeding 3000 mm³ as humane endpoints.

CHO/HER2 cells were suspended in BD Matrigel Matrix Growth Factor Reduced (BD Biosciences, San Jose, CA, USA). Then, BALB/c nude mice (Jackson Laboratory Japan, Kanagawa, Japan) were injected subcutaneously in the left flank with 100 µL of the suspension (5 × 10⁶ cells). On days 9 and 16 post-inoculation, 100 µg of H₂Mab-250-mG_{2a} (n = 8), tras-mG_{2a} (n = 8), or control mouse IgG_{2a} (PMab-231; n = 8) in 100 µL PBS was intraperitoneally injected.

For evaluation of H₂Mab-250-hG₁ and trastuzumab, we injected the mice with 100 µg of H₂Mab-250-hG₁ (n = 8), trastuzumab (n = 8), or control human IgG (n = 8) in 100 µL of PBS through intraperitoneal injection on days 7, 14, and 21 post-inoculation. Furthermore, human NK cells (8.0 × 10⁵ cells, Takara Bio, Inc.) were injected near the tumors subcutaneously on same days as the mAbs injection.

The tumor volume was calculated using the following formula: volume = W² × L/2, where W is the short diameter and L is the long diameter. All the mice were euthanized by cervical dislocation.

Statistical analyses were performed using GraphPad PRISM 6 (GraphPad Software, Inc., La Jolla, CA, USA).

4.6. Pharmacokinetics of H₂Mab-250-hG₁ and Trastuzumab

HER2 ectodomain [34] was immobilized on Nunc Maxisorp 96-well immunoplates (Thermo Fisher Scientific Inc.) at a concentration of 1 µg/mL for 30 min at 37 °C. After washing with PBS containing 0.05% (*v/v*) Tween 20 (PBST; Nacalai Tesque, Inc.), the wells were blocked with 1% (*w/v*) bovine serum albumin (BSA)-containing PBST for 30 min at 37 °C. To make a standard curve, the serially diluted H₂Mab-250-hG₁ and trastuzumab (0.00064–10 µg/mL) were added to each well, followed by peroxidase-conjugated anti-human Fc (1:3000 diluted; Sigma-Aldrich Corp.). The enzymatic reactions were conducted using ELISA POD Substrate TMB Kit (Nacalai Tesque, Inc.), followed by the measurement of the optical density at 655 nm, using an iMark microplate reader (Bio-Rad Laboratories, Inc., Berkeley, CA, USA). The standard curve was produced using GraphPad PRISM 6. H₂Mab-250-hG₁ and trastuzumab (100 µg/mouse, *n* = 3) were intraperitoneally injected and the serums were collected from day 0 (4 h after injection) to 10. The concentration of mAbs was determined as described above. The half-life of the mAbs was calculated as described previously [53].

Supplementary Materials: The following supporting information can be downloaded at <https://www.mdpi.com/article/10.3390/ijms25158386/s1>.

Author Contributions: H.S., T.O. and T.T. performed the experiments. M.K.K. and Y.K. designed the experiments. H.S., T.T. and Y.K. analyzed the data. H.S. and Y.K. wrote the manuscript. All authors have read and agreed to the published version of the manuscript.

Funding: This research was supported in part by the Japan Agency for Medical Research and Development (AMED) under the following grant numbers: 24am0521010 (to Y.K.), JP23ama121008 (to Y.K.), JP23am0401013 (to Y.K.), JP23bm1123027 (to Y.K.), JP23ck0106730 (to Y.K.), JP18am0301010 (to Y.K.), and JP21am0101078 (to Y.K.).

Institutional Review Board Statement: The Institutional Committee for Experiments of the Institute of Microbial Chemistry approved the animal experiment to examine the antitumor effect (approval no. 2023-066 and 2023-074).

Informed Consent Statement: Not applicable.

Data Availability Statement: The data presented in this study are available in the article.

Conflicts of Interest: The authors declare no conflicts of interest.

References

1. Yarden, Y.; Sliwkowski, M.X. Untangling the ErbB signalling network. *Nat. Rev. Mol. Cell Biol.* **2001**, *2*, 127–137. [[CrossRef](#)] [[PubMed](#)]
2. Slamon, D.J.; Clark, G.M.; Wong, S.G.; Levin, W.J.; Ullrich, A.; McGuire, W.L. Human breast cancer: Correlation of relapse and survival with amplification of the HER-2/neu oncogene. *Science* **1987**, *235*, 177–182. [[CrossRef](#)] [[PubMed](#)]
3. Van Cutsem, E.; Bang, Y.J.; Feng-Yi, F.; Xu, J.M.; Lee, K.W.; Jiao, S.C.; Chong, J.L.; López-Sánchez, R.I.; Price, T.; Gladkov, O.; et al. HER2 screening data from ToGA: Targeting HER2 in gastric and gastroesophageal junction cancer. *Gastric Cancer* **2015**, *18*, 476–484. [[CrossRef](#)] [[PubMed](#)]
4. Tsao, L.C.; Force, J.; Hartman, Z.C. Mechanisms of Therapeutic Antitumor Monoclonal Antibodies. *Cancer Res.* **2021**, *81*, 4641–4651. [[CrossRef](#)] [[PubMed](#)]
5. Gschwind, A.; Fischer, O.M.; Ullrich, A. The discovery of receptor tyrosine kinases: Targets for cancer therapy. *Nat. Rev. Cancer* **2004**, *4*, 361–370. [[CrossRef](#)] [[PubMed](#)]
6. Slamon, D.J.; Leyland-Jones, B.; Shak, S.; Fuchs, H.; Paton, V.; Bajamonde, A.; Fleming, T.; Eiermann, W.; Wolter, J.; Pegram, M.; et al. Use of chemotherapy plus a monoclonal antibody against HER2 for metastatic breast cancer that overexpresses HER2. *N. Engl. J. Med.* **2001**, *344*, 783–792. [[CrossRef](#)] [[PubMed](#)]
7. Maadi, H.; Soheilifar, M.H.; Choi, W.S.; Moshtaghian, A.; Wang, Z. Trastuzumab Mechanism of Action; 20 Years of Research to Unravel a Dilemma. *Cancers* **2021**, *13*, 3540. [[CrossRef](#)]
8. Cardoso, F.; Paluch-Shimon, S.; Senkus, E.; Curigliano, G.; Aapro, M.S.; André, F.; Barrios, C.H.; Bergh, J.; Bhattacharyya, G.S.; Biganzoli, L.; et al. 5th ESO-ESMO international consensus guidelines for advanced breast cancer (ABC 5). *Ann. Oncol.* **2020**, *31*, 1623–1649. [[CrossRef](#)]
9. Mark, C.; Lee, J.S.; Cui, X.; Yuan, Y. Antibody-Drug Conjugates in Breast Cancer: Current Status and Future Directions. *Int. J. Mol. Sci.* **2023**, *24*, 13726. [[CrossRef](#)]

10. Modi, S.; Saura, C.; Yamashita, T.; Park, Y.H.; Kim, S.B.; Tamura, K.; Andre, F.; Iwata, H.; Ito, Y.; Tsurutani, J.; et al. Trastuzumab Deruxtecan in Previously Treated HER2-Positive Breast Cancer. *N. Engl. J. Med.* **2020**, *382*, 610–621. [[CrossRef](#)]
11. Shitara, K.; Bang, Y.J.; Iwasa, S.; Sugimoto, N.; Ryu, M.H.; Sakai, D.; Chung, H.C.; Kawakami, H.; Yabusaki, H.; Lee, J.; et al. Trastuzumab Deruxtecan in Previously Treated HER2-Positive Gastric Cancer. *N. Engl. J. Med.* **2020**, *382*, 2419–2430. [[CrossRef](#)]
12. Modi, S.; Jacot, W.; Yamashita, T.; Sohn, J.; Vidal, M.; Tokunaga, E.; Tsurutani, J.; Ueno, N.T.; Prat, A.; Chae, Y.S.; et al. Trastuzumab Deruxtecan in Previously Treated HER2-Low Advanced Breast Cancer. *N. Engl. J. Med.* **2022**, *387*, 9–20. [[CrossRef](#)] [[PubMed](#)]
13. Li, B.T.; Smit, E.F.; Goto, Y.; Nakagawa, K.; Udagawa, H.; Mazières, J.; Nagasaka, M.; Bazhenova, L.; Saltos, A.N.; Felip, E.; et al. Trastuzumab Deruxtecan in HER2-Mutant Non-Small-Cell Lung Cancer. *N. Engl. J. Med.* **2022**, *386*, 241–251. [[CrossRef](#)] [[PubMed](#)]
14. Mercogliano, M.F.; Bruni, S.; Mauro, F.L.; Schillaci, R. Emerging Targeted Therapies for HER2-Positive Breast Cancer. *Cancers* **2023**, *15*, 1987. [[CrossRef](#)]
15. Galvez-Cancino, F.; Simpson, A.P.; Costoya, C.; Matos, I.; Qian, D.; Peggs, K.S.; Litchfield, K.; Quezada, S.A. Fcγ receptors and immunomodulatory antibodies in cancer. *Nat. Rev. Cancer* **2024**, *24*, 51–71. [[CrossRef](#)]
16. Pereira, N.A.; Chan, K.F.; Lin, P.C.; Song, Z. The “less-is-more” in therapeutic antibodies: Afucosylated anti-cancer antibodies with enhanced antibody-dependent cellular cytotoxicity. *MAbs* **2018**, *10*, 693–711. [[CrossRef](#)]
17. Shinkawa, T.; Nakamura, K.; Yamane, N.; Shoji-Hosaka, E.; Kanda, Y.; Sakurada, M.; Uchida, K.; Anazawa, H.; Satoh, M.; Yamasaki, M.; et al. The absence of fucose but not the presence of galactose or bisecting N-acetylglucosamine of human IgG1 complex-type oligosaccharides shows the critical role of enhancing antibody-dependent cellular cytotoxicity. *J. Biol. Chem.* **2003**, *278*, 3466–3473. [[CrossRef](#)]
18. Niwa, R.; Shoji-Hosaka, E.; Sakurada, M.; Shinkawa, T.; Uchida, K.; Nakamura, K.; Matsushima, K.; Ueda, R.; Hanai, N.; Shitara, K. Defucosylated chimeric anti-CC chemokine receptor 4 IgG1 with enhanced antibody-dependent cellular cytotoxicity shows potent therapeutic activity to T-cell leukemia and lymphoma. *Cancer Res.* **2004**, *64*, 2127–2133. [[CrossRef](#)] [[PubMed](#)]
19. Yamane-Ohnuki, N.; Kinoshita, S.; Inoue-Urakubo, M.; Kusunoki, M.; Iida, S.; Nakano, R.; Wakitani, M.; Niwa, R.; Sakurada, M.; Uchida, K.; et al. Establishment of FUT8 knockout Chinese hamster ovary cells: An ideal host cell line for producing completely defucosylated antibodies with enhanced antibody-dependent cellular cytotoxicity. *Biotechnol. Bioeng.* **2004**, *87*, 614–622. [[CrossRef](#)]
20. Golay, J.; Taylor, R.P. The Role of Complement in the Mechanism of Action of Therapeutic Anti-Cancer mAbs. *Antibodies* **2020**, *9*, 58. [[CrossRef](#)]
21. Reis, E.S.; Mastellos, D.C.; Ricklin, D.; Mantovani, A.; Lambris, J.D. Complement in cancer: Untangling an intricate relationship. *Nat. Rev. Immunol.* **2018**, *18*, 5–18. [[CrossRef](#)] [[PubMed](#)]
22. Taylor, R.P.; Lindorfer, M.A. Cytotoxic mechanisms of immunotherapy: Harnessing complement in the action of anti-tumor monoclonal antibodies. *Semin. Immunol.* **2016**, *28*, 309–316. [[CrossRef](#)] [[PubMed](#)]
23. Reff, M.E.; Carner, K.; Chambers, K.S.; Chinn, P.C.; Leonard, J.E.; Raab, R.; Newman, R.A.; Hanna, N.; Anderson, D.R. Depletion of B cells in vivo by a chimeric mouse human monoclonal antibody to CD20. *Blood* **1994**, *83*, 435–445. [[CrossRef](#)] [[PubMed](#)]
24. de Weers, M.; Tai, Y.T.; van der Veer, M.S.; Bakker, J.M.; Vink, T.; Jacobs, D.C.; Oomen, L.A.; Peipp, M.; Valerius, T.; Slootstra, J.W.; et al. Daratumumab, a novel therapeutic human CD38 monoclonal antibody, induces killing of multiple myeloma and other hematological tumors. *J. Immunol.* **2011**, *186*, 1840–1848. [[CrossRef](#)] [[PubMed](#)]
25. Zent, C.S.; Secreto, C.R.; LaPlant, B.R.; Bone, N.D.; Call, T.G.; Shanafelt, T.D.; Jelinek, D.F.; Tschumper, R.C.; Kay, N.E. Direct and complement dependent cytotoxicity in CLL cells from patients with high-risk early-intermediate stage chronic lymphocytic leukemia (CLL) treated with alemtuzumab and rituximab. *Leuk. Res.* **2008**, *32*, 1849–1856. [[CrossRef](#)] [[PubMed](#)]
26. Schmutte, I.; Laumonier, Y.; Köhl, J. Anaphylatoxins coordinate innate and adaptive immune responses in allergic asthma. *Semin. Immunol.* **2013**, *25*, 2–11. [[CrossRef](#)] [[PubMed](#)]
27. Carroll, M.C.; Isenman, D.E. Regulation of humoral immunity by complement. *Immunity* **2012**, *37*, 199–207. [[CrossRef](#)] [[PubMed](#)]
28. Soares, L.R.; Vilbert, M.; Rosa, V.D.L.; Oliveira, J.L.; Deus, M.M.; Freitas-Junior, R. Incidence of interstitial lung disease and cardiotoxicity with trastuzumab deruxtecan in breast cancer patients: A systematic review and single-arm meta-analysis. *ESMO Open* **2023**, *8*, 101613. [[CrossRef](#)] [[PubMed](#)]
29. Copeland-Halperin, R.S.; Liu, J.E.; Yu, A.F. Cardiotoxicity of HER2-targeted therapies. *Curr. Opin. Cardiol.* **2019**, *34*, 451–458. [[CrossRef](#)] [[PubMed](#)]
30. Lee, K.F.; Simon, H.; Chen, H.; Bates, B.; Hung, M.C.; Hauser, C. Requirement for neuregulin receptor erbB2 in neural and cardiac development. *Nature* **1995**, *378*, 394–398. [[CrossRef](#)]
31. Crone, S.A.; Zhao, Y.Y.; Fan, L.; Gu, Y.; Minamisawa, S.; Liu, Y.; Peterson, K.L.; Chen, J.; Kahn, R.; Condorelli, G.; et al. ErbB2 is essential in the prevention of dilated cardiomyopathy. *Nat. Med.* **2002**, *8*, 459–465. [[CrossRef](#)] [[PubMed](#)]
32. Arimori, T.; Mihara, E.; Suzuki, H.; Ohishi, T.; Tanaka, T.; Kaneko, M.K.; Takagi, J.; Kato, Y. Locally misfolded HER2 expressed on cancer cells is a promising target for development of cancer-specific antibodies. *Structure* **2024**, *32*, 536–549.e5. [[CrossRef](#)] [[PubMed](#)]
33. Kaneko, M.K.; Suzuki, H.; Kato, Y. Establishment of a Novel Cancer-Specific Anti-HER2 Monoclonal Antibody H(2)Mab-250/H(2)CasMab-2 for Breast Cancers. *Monoclon. Antib. Immunodiagn. Immunother.* **2024**, *43*, 35–43. [[CrossRef](#)] [[PubMed](#)]
34. Kaneko, M.K.; Suzuki, H.; Ohishi, T.; Nakamura, T.; Tanaka, T.; Kato, Y. A Cancer-Specific Monoclonal Antibody against HER2 Exerts Antitumor Activities in Human Breast Cancer Xenograft Models. *Int. J. Mol. Sci.* **2024**, *25*, 1941. [[CrossRef](#)] [[PubMed](#)]
35. Suzuki, H.; Ohishi, T.; Tanaka, T.; Kaneko, M.K.; Kato, Y. A Cancer-Specific Monoclonal Antibody against Podocalyxin Exerted Antitumor Activities in Pancreatic Cancer Xenografts. *Int. J. Mol. Sci.* **2023**, *25*, 161. [[CrossRef](#)] [[PubMed](#)]

36. Kato, Y.; Kaneko, M.K. A cancer-specific monoclonal antibody recognizes the aberrantly glycosylated podoplanin. *Sci. Rep.* **2014**, *4*, 5924. [[CrossRef](#)] [[PubMed](#)]
37. Yamada, S.; Ogasawara, S.; Kaneko, M.K.; Kato, Y. LpMab-23: A Cancer-Specific Monoclonal Antibody against Human Podoplanin. *Monoclon. Antib. Immunodiagn. Immunother.* **2017**, *36*, 72–76. [[CrossRef](#)] [[PubMed](#)]
38. Merle, N.S.; Church, S.E.; Fremeaux-Bacchi, V.; Roumenina, L.T. Complement System Part I—Molecular Mechanisms of Activation and Regulation. *Front. Immunol.* **2015**, *6*, 262. [[CrossRef](#)] [[PubMed](#)]
39. Hiemstra, I.H.; Santegoets, K.C.M.; Janmaat, M.L.; De Goeij, B.; Ten Hagen, W.; van Dooremalen, S.; Boross, P.; van den Brakel, J.; Bosgra, S.; Andringa, G.; et al. Preclinical anti-tumour activity of HexaBody-CD38, a next-generation CD38 antibody with superior complement-dependent cytotoxic activity. *eBioMedicine* **2023**, *93*, 104663. [[CrossRef](#)]
40. de Jong, R.N.; Beurskens, F.J.; Verploegen, S.; Strumane, K.; van Kampen, M.D.; Voorhorst, M.; Horstman, W.; Engelberts, P.J.; Oostindie, S.C.; Wang, G.; et al. A Novel Platform for the Potentiation of Therapeutic Antibodies Based on Antigen-Dependent Formation of IgG Hexamers at the Cell Surface. *PLoS Biol.* **2016**, *14*, e1002344. [[CrossRef](#)]
41. Mamidi, S.; Cinci, M.; Hasmann, M.; Fehring, V.; Kirschfink, M. Lipoplex mediated silencing of membrane regulators (CD46, CD55 and CD59) enhances complement-dependent anti-tumor activity of trastuzumab and pertuzumab. *Mol. Oncol.* **2013**, *7*, 580–594. [[CrossRef](#)] [[PubMed](#)]
42. Wang, Y.; Yang, Y.J.; Wang, Z.; Liao, J.; Liu, M.; Zhong, X.R.; Zheng, H.; Wang, Y.P. CD55 and CD59 expression protects HER2-overexpressing breast cancer cells from trastuzumab-induced complement-dependent cytotoxicity. *Oncol. Lett.* **2017**, *14*, 2961–2969. [[CrossRef](#)] [[PubMed](#)]
43. Weisser, N.E.; Sanches, M.; Escobar-Cabrera, E.; O’Toole, J.; Whalen, E.; Chan, P.W.Y.; Wickman, G.; Abraham, L.; Choi, K.; Harbourne, B.; et al. An anti-HER2 biparatopic antibody that induces unique HER2 clustering and complement-dependent cytotoxicity. *Nat. Commun.* **2023**, *14*, 1394. [[CrossRef](#)] [[PubMed](#)]
44. Diebold, C.A.; Beurskens, F.J.; de Jong, R.N.; Koning, R.I.; Strumane, K.; Lindorfer, M.A.; Voorhorst, M.; Ugurlar, D.; Rosati, S.; Heck, A.J.; et al. Complement is activated by IgG hexamers assembled at the cell surface. *Science* **2014**, *343*, 1260–1263. [[CrossRef](#)] [[PubMed](#)]
45. Zipfel, P.F.; Skerka, C. Complement regulators and inhibitory proteins. *Nat. Rev. Immunol.* **2009**, *9*, 729–740. [[CrossRef](#)] [[PubMed](#)]
46. Okroj, M.; Hsu, Y.F.; Ajona, D.; Pio, R.; Blom, A.M. Non-small cell lung cancer cells produce a functional set of complement factor I and its soluble cofactors. *Mol. Immunol.* **2008**, *45*, 169–179. [[CrossRef](#)] [[PubMed](#)]
47. Spiller, O.B.; Criado-García, O.; Rodríguez De Córdoba, S.; Morgan, B.P. Cytokine-mediated up-regulation of CD55 and CD59 protects human hepatoma cells from complement attack. *Clin. Exp. Immunol.* **2000**, *121*, 234–241. [[CrossRef](#)] [[PubMed](#)]
48. Sherbenou, D.W.; Aftab, B.T.; Su, Y.; Behrens, C.R.; Wiita, A.; Logan, A.C.; Acosta-Alvear, D.; Hann, B.C.; Walter, P.; Shuman, M.A.; et al. Antibody-drug conjugate targeting CD46 eliminates multiple myeloma cells. *J. Clin. Investig.* **2016**, *126*, 4640–4653. [[CrossRef](#)] [[PubMed](#)]
49. Hu, W.; Ge, X.; You, T.; Xu, T.; Zhang, J.; Wu, G.; Peng, Z.; Chorev, M.; Aktas, B.H.; Halperin, J.A.; et al. Human CD59 inhibitor sensitizes rituximab-resistant lymphoma cells to complement-mediated cytotoxicity. *Cancer Res.* **2011**, *71*, 2298–2307. [[CrossRef](#)]
50. Geis, N.; Zell, S.; Rutz, R.; Li, W.; Giese, T.; Mamidi, S.; Schultz, S.; Kirschfink, M. Inhibition of membrane complement inhibitor expression (CD46, CD55, CD59) by siRNA sensitizes tumor cells to complement attack in vitro. *Curr. Cancer Drug Targets* **2010**, *10*, 922–931. [[CrossRef](#)]
51. Imai, M.; Ohta, R.; Varela, J.C.; Song, H.; Tomlinson, S. Enhancement of antibody-dependent mechanisms of tumor cell lysis by a targeted activator of complement. *Cancer Res.* **2007**, *67*, 9535–9541. [[CrossRef](#)] [[PubMed](#)]
52. Furusawa, Y.; Kaneko, M.K.; Nakamura, T.; Itai, S.; Fukui, M.; Harada, H.; Yamada, S.; Kato, Y. Establishment of a Monoclonal Antibody PMab-231 for Tiger Podoplanin. *Monoclon. Antib. Immunodiagn. Immunother.* **2019**, *38*, 89–95. [[CrossRef](#)] [[PubMed](#)]
53. Rowland, M.; Tozer, T. *Clinical Pharmacokinetics and Pharmacodynamics: Concepts and Applications*, 4th ed.; Wolters Kluwer/Lippincott Williams & Wilkins: Philadelphia, PA, USA, 2010.

Disclaimer/Publisher’s Note: The statements, opinions and data contained in all publications are solely those of the individual author(s) and contributor(s) and not of MDPI and/or the editor(s). MDPI and/or the editor(s) disclaim responsibility for any injury to people or property resulting from any ideas, methods, instructions or products referred to in the content.